

# Low energy electronic states in spheroidal fullerenes

M. Pudlak<sup>a</sup>, R. Pincak<sup>a,b</sup> and V.A. Osipov<sup>b</sup>

<sup>a</sup>*Institute of Experimental Physics, Slovak Academy of Sciences, Watsonova 47,043 53 Kosice, Slovak Republic*

<sup>b</sup>*Joint Institute for Nuclear Research, Bogoliubov Laboratory of Theoretical Physics, 141980 Dubna, Moscow region, Russia*  
*e-mail: pudlak@saske.sk, pincak@saske.sk, osipov@thsun1.jinr.ru*

(March 23, 2022)

The field-theory model is proposed to study the electronic states near the Fermi energy in spheroidal fullerenes. The low energy electronic wavefunctions obey a two-dimensional Dirac equation on a spheroid with two kinds of gauge fluxes taken into account. The first one is so-called K spin flux which describes the exchange of two different Dirac spinors in the presence of a conical singularity. The second flux (included in a form of the Dirac monopole field) is a variant of the effective field approximation for elastic flow due to twelve disclination defects through the surface of a spheroid. We consider the case of a slightly elliptically deformed sphere which allows us to apply the perturbation scheme. It is shown exactly how a small deformation of spherical fullerenes provokes an appearance of fine structure in the electronic energy spectrum as compared to the spherical case. In particular, two quasi-zero modes in addition to the true zero mode are predicted to emerge in spheroidal fullerenes. An additional 'hyperfine' splitting of the levels (except the quasi-zero-mode states) is found.

## I. INTRODUCTION

Geometry, topological defects and the peculiarity of graphene lattice have a pronounced effect on the electronic structure of fullerene molecules. The most extensively studied  $C_{60}$  molecule is an example of a spherical fullerene nicknamed a "soccer ball" [1]. The family of icosahedral spherical fullerenes is described by the formula  $20(n^2 + nl + l^2)$  with integer  $n$  and  $l$ . Other fullerenes are either slightly (as  $C_{70}$ ) or remarkably deformed and their general nickname is a "rugby ball". The electronic structure of  $C_{70}$  cluster of  $D_{5h}$  geometry has been studied in [2] by using the local-density approximation in the density-functional theory. It was clearly shown that the spheroidal geometry is of a decisive importance for observed peculiarities in electronic states of the  $C_{70}$ . What is important, the calculated energy levels were found to be in good agreement with photoemission experiments.

Among different theoretical approaches to describe graphene compositions such as nanotubes, cones, nanohorns and fullerenes the continuum models play a special role. Indeed, the continuum models allow us to describe some integral features of similar carbon structures. For instance, in the case of the spherical fullerenes the obtained results can be extended on the whole  $60n^2$  family. On the other hand, the continuum description gives an important information about long-distance physics which is difficult to get within other approaches like, e.g., widely-used tight-binding models. In addition, the continuum models are useful for clarification of pure topological effects such as an appearance of the Aharonov-Bohm phase and anomalous Landau levels (see, e.g., Refs. [3–5]).

It should be noted that the formulation of any continuum model begins from the description of a graphite sheet (graphene) (see, e.g., [6–11]). The models which involve the influence of both geometry and topological defects on the electronic structure by boundary conditions were developed in Refs. [12,13]. A different variant of the continuum model within the effective-mass description for fullerene near one pentagonal defect was suggested in Refs. [14,15]. There are attempts to describe electronic structure of the graphene compositions by the Dirac-Weyl equations on the curved surfaces where the structure of the graphite with pentagonal rings taken into account is imposed with the help of the so-called K spin contribution [16,3]. In the case of spherical geometry, this is realized by introducing an effective field due to magnetic monopole placed at the center of a sphere [16]. In the present paper we use a similar approach. The difference is that we consider also the elastic contribution. Indeed, pentagonal rings being the disclination defects are the sources of additional strains in the hexagonal lattice. Moreover, the disclinations are topological defects and the elastic flow due to a disclination is determined by the topological Frank index. For this reason, this contribution exists even within the so-called "inextensional" limit which is rather commonly used in description of graphene compositions (see, e.g., [17]).

Recently, in the framework of a continuum approach the exact analytical solution for the low energy electronic states in icosahedral spherical fullerenes has been found [18]. The case of elliptically deformed fullerenes was studied in [19] where some numerical results were presented. In this paper, we suggest a similar to [18] model with the

Dirac monopole instead of 't Hooft-Polyakov monopole for describing elastic fields. We consider a slightly elliptically deformed sphere with the eccentricity of the spheroid  $e \ll 1$ . In this case, by analogy with [20] we use the spherical representation for the eigenstates, with the slight asphericity considered as a perturbation. This allows us to find explicitly the low-lying electronic spectrum for spheroidal fullerenes.

## II. THE MODEL

Our studies cover spherical molecules which are slightly elliptically deformed. Let us start with introducing spheroidal coordinates and writing down the Dirac operator for free massless fermions on the Riemannian spheroid  $S^2$ . The Euler's theorem for graphene requires the presence of twelve pentagons to get the closed molecule. In a spirit of a continuum description we will extend the Dirac operator by introducing the Dirac monopole field inside the spheroid to simulate the elastic vortices due to twelve pentagonal defects. The K spin flux which describes the exchange of two different Dirac spinors in the presence of a conical singularity will also be included in a form of 't Hooft-Polyakov monopole.

To incorporate fermions on the curved background, we need a set of orthonormal frames  $\{e_\alpha\}$ , which yield the same metric,  $g_{\mu\nu}$ , related to each other by the local  $SO(2)$  rotation,

$$e_\alpha \rightarrow e'_\alpha = \Lambda_\alpha^\beta e_\beta, \quad \Lambda_\alpha^\beta \in SO(2).$$

It then follows that  $g_{\mu\nu} = e_\mu^\alpha e_\nu^\beta \delta_{\alpha\beta}$  where  $e_\alpha^\mu$  is the zweibein, with the orthonormal frame indices being  $\alpha, \beta = \{1, 2\}$ , and the coordinate indices  $\mu, \nu = \{1, 2\}$ . As usual, to ensure that physical observables are independent of a particular choice of the zweibein fields, a local  $so(2)$  valued gauge field  $\omega_\mu$  is to be introduced. The gauge field of the local Lorentz group is known as a spin connection. The Dirac equation on a surface  $\Sigma$  in the presence of the abelian magnetic monopole field  $A_\mu$  is written as [21]

$$i\gamma^\alpha e_\alpha^\mu [\nabla_\mu - iA_\mu]\psi = E\psi, \quad (1)$$

where  $\nabla_\mu = \partial_\mu + \Omega_\mu$  with

$$\Omega_\mu = \frac{1}{8}\omega_\mu^{\alpha\beta}[\gamma_\alpha, \gamma_\beta], \quad (2)$$

being the spin connection term in the spinor representation.

The elliptically deformed sphere or a spheroid

$$\frac{x^2}{a^2} + \frac{y^2}{a^2} + \frac{z^2}{c^2} = 1, \quad (3)$$

may be parameterized by two spherical angles  $q^1 = \phi$ ,  $q^2 = \theta$  that are related to the Cartesian coordinates  $x, y, z$  as follows

$$x = a \sin \theta \cos \phi; \quad y = a \sin \theta \sin \phi; \quad z = c \cos \theta. \quad (4)$$

The nonzero components of the metric tensor for spheroid are

$$g_{\phi\phi} = a^2 \sin^2 \theta; \quad g_{\theta\theta} = a^2 \cos^2 \theta + c^2 \sin^2 \theta, \quad (5)$$

where  $a, c \geq 0$ ,  $0 \leq \theta \leq \pi$ ,  $0 \leq \phi < 2\pi$ . Accordingly, orthonormal frame on spheroid is

$$e_1 = \frac{1}{a \sin \theta} \partial_\phi; \quad e_2 = \frac{1}{\sqrt{a^2 \cos^2 \theta + c^2 \sin^2 \theta}} \partial_\theta, \quad (6)$$

and dual frame reads

$$e^1 = a \sin \theta d\phi; \quad e^2 = \sqrt{a^2 \cos^2 \theta + c^2 \sin^2 \theta} d\theta. \quad (7)$$

A general representation for zweibeins is found to be

$$e^1_\phi = a \sin \theta; \quad e^1_\theta = 0; \quad e^2_\phi = 0; \quad e^2_\theta = \sqrt{a^2 \cos^2 \theta + c^2 \sin^2 \theta}. \quad (8)$$

Notice that  $e^\mu{}_\alpha$  is the inverse of  $e^\alpha{}_\mu$ . The Riemannian connection with respect to the orthonormal frame is written as [22,23]

$$de^1 = -\omega^1{}_2 \wedge e^2 = \frac{a \cos \theta}{\sqrt{a^2 \cos^2 \theta + c^2 \sin^2 \theta}} d\phi \wedge e^2, \quad (9)$$

$$de^2 = -\omega^2{}_1 \wedge e^1 = 0. \quad (10)$$

Here  $\wedge$  denotes the exterior product and  $d$  is the exterior derivative. From Eqs.(9) and (10) we get the Riemannian connection in the form

$$\omega^1{}_{\phi 2} = -\omega^2{}_{\phi 1} = \frac{a \cos \theta}{\sqrt{a^2 \cos^2 \theta + c^2 \sin^2 \theta}}; \quad \omega^1{}_{\theta 2} = \omega^2{}_{\theta 1} = 0. \quad (11)$$

We assume that the eccentricity of the spheroid  $e = \sqrt{1 - (c/a)^2}$  is small enough. In this case, one can write down  $c = a + \delta a$  where  $\delta$  ( $|\delta| \ll 1$ ) is a small dimensionless parameter characterizing the spheroidal deformation from the sphere. So, we can follow the perturbation scheme using  $\delta$  as the perturbation parameter.

Within the perturbation scheme, the spin connection coefficients are rewritten as

$$\omega^1{}_{\phi 2} = -\omega^2{}_{\phi 1} \approx \cos \theta (1 - \delta \sin^2 \theta). \quad (12)$$

The inclusion of the K-spin connection can be performed by considering two Dirac spinors as the two components of an  $SU(2)$  color doublet  $\psi = (\psi_\uparrow \psi_\downarrow)^T$  (see Ref. [16] for details). In this case, the interaction with the color magnetic fields in a form of nonabelian magnetic flux ('t Hooft'-Polyakov monopole) is responsible for the exchange of the two Dirac spinors which in turn corresponds to the interchange of Fermi points. As was shown in Ref. [24], the Dirac equation for  $\psi$  can be reduced to two decoupled equations for  $\psi_\uparrow$  and  $\psi_\downarrow$ , which include an Abelian monopole of opposite charge,  $g = \pm 3/2$ .

The elastic flow through a surface due to a disclination has a vortex-like structure [14] and can be described by Abelian gauge field  $W_\mu$ . Similarly to Ref. [16], we replace the fields of twelve disclinations by the effective field of the magnetic monopole of charge  $G$  located at the center of the spheroid. The circulation of this field is determined by the Frank index, which is the topological characteristic of a disclination. Trying to avoid an extension of the group we will consider the case of the Dirac monopole. The another possibility is to introduce the non-Abelian 't Hooft-Polyakov monopole (see Ref. [18]). As is known, the vector potential  $W_\mu$  around the Dirac monopole have singularities. To escape introducing singularities in the coordinate system let us divide the spheroid (similarly as it was done for the sphere in [25]) into two regions,  $R_N$  and  $R_S$ , and define a vector potential  $A_\mu^N$  in  $R_N$  and a vector potential  $A_\mu^S$  in  $R_S$ . Notice that  $A_\mu$  includes both gauge fields. One has

$$R_N : \quad 0 \leq \theta < \frac{\pi}{2} + \Delta; \quad 0 \leq \phi < 2\pi, \quad (13)$$

$$R_S : \quad \frac{\pi}{2} - \Delta < \theta \leq \pi; \quad 0 \leq \phi < 2\pi, \quad (14)$$

$$R_{NS} : \quad \frac{\pi}{2} - \Delta < \theta < \frac{\pi}{2} + \Delta; \quad 0 \leq \phi < 2\pi, \quad (overlap) \quad (15)$$

where  $\Delta$  is chosen from the interval  $0 < \Delta \leq \pi/2$ . In spheroidal coordinates (5) the only nonzero components of  $A_\mu$  are found to be

$$A_\phi^N \approx g \cos \theta (1 + \delta \sin^2 \theta) + G(1 - \cos \theta) - \delta G \sin^2 \theta \cos \theta, \quad (16)$$

$$A_\phi^S \approx g \cos \theta (1 + \delta \sin^2 \theta) - G(1 + \cos \theta) - \delta G \sin^2 \theta \cos \theta, \quad (17)$$

where the terms of an order of  $\delta^2$  and higher are dropped. In the overlapping region the potentials  $A_\phi^N$  and  $A_\phi^S$  are connected by the gauge transformation

$$A_\phi^N = A_\phi^S + i S_{NS} \partial_\phi S_{NS}^{-1}, \quad (18)$$

where

$$S_{NS} = e^{2iG\phi}$$

is the phase factor. The wavefunctions in the overlap  $R_{NS}$  are connected by

$$\psi_N = S_{NS}\psi_S, \quad (19)$$

where  $\psi_N$  and  $\psi_S$  are the spinors in  $R_N$  and  $R_S$ , respectively. Since  $S_{NS}$  must be single-valued [26],  $2G$  takes integer values. Notice that the total flux due to Dirac monopole in (16) and (17) is equal to  $4\pi G$ . What is important, there is no contribution from the terms with  $\delta$ . In our case, the total flux describes a sum of elastic fluxes due to twelve disclinations, so that the total flux (the modulus of the total Frank vector) is equal to  $12 \times \pi/3 = 4\pi$ . Therefore, one obtains  $G = 1$ .

Let us consider the region  $R_N$ . The Dirac operator for spheroidal fullerenes with monopole fields inside the spheroid takes the following form:

$$\hat{\mathcal{D}} = \hat{\mathcal{D}}_0 + \delta\hat{\mathcal{D}}_1, \quad (20)$$

where

$$\hat{\mathcal{D}}_0 = i\gamma_2 \frac{1}{a} (\partial_\theta + \frac{\cot \theta}{2}) + i \frac{\gamma_1}{a \sin \theta} (\partial_\phi - iG(1 - \cos \theta) - ig \cos \theta),$$

is the Dirac operator for spherical fullerenes and

$$\hat{\mathcal{D}}_1 = -i\gamma_1 \frac{1}{a \sin \theta} \left[ \frac{\cos \theta \sin^2 \theta}{2} \gamma_1 \gamma_2 + i(g - G) \sin^2 \theta \cos \theta \right] - i\gamma_2 \frac{\sin^2 \theta}{a} \partial_\theta,$$

is the perturbation part of the spheroidal Dirac operator. This operator is hermitian on the spheroid. Actually, we consider the Dirac operator on the spheroid as a perturbation of the Dirac operator on the sphere (cf. [20]). For this reason,  $\hat{\mathcal{D}}$  should be transformed into the operator which is hermitian on the sphere. After straightforward calculations one obtains that the form of the operator  $\hat{\mathcal{D}}_0$  remains the same while  $\hat{\mathcal{D}}_1$  is written as

$$\hat{\mathcal{D}}_1 = -\frac{\gamma_1}{a} \sin \theta (j - 2m \cos \theta). \quad (21)$$

Let us turn back to Eq.(1) and formulate the eigenvalue problem for Dirac operator on the spheroid. Since a surface is a two dimensional space, the Dirac matrices can be chosen to be the Pauli matrices,  $\gamma_1 = -\sigma_2$ ,  $\gamma_2 = -\sigma_1$ . We can restrict our consideration to only one of spinors, say to  $\psi_\uparrow$ . By using the substitution

$$\begin{pmatrix} \psi_A \\ \psi_B \end{pmatrix} = \sum_j \frac{e^{i(j+G)\phi}}{\sqrt{2\pi}} \begin{pmatrix} u_j(\theta) \\ v_j(\theta) \end{pmatrix}, j = 0, \pm 1, \pm 2, \dots \quad (22)$$

we obtain the Dirac equations for the spinor functions  $u_j$  and  $v_j$  in the form

$$\left( -i\sigma_1 \frac{1}{a} (\partial_\theta + \frac{\cot \theta}{2}) + \frac{\sigma_2}{a \sin \theta} (j - m \cos \theta) + \delta\hat{\mathcal{D}}_1 \right) \begin{pmatrix} u_j(\theta) \\ v_j(\theta) \end{pmatrix} = E \begin{pmatrix} u_j(\theta) \\ v_j(\theta) \end{pmatrix}, \quad (23)$$

where  $m = g - G$ . To first order in  $\delta$ , the square of the spheroidal Dirac operator is written as  $\hat{\mathcal{D}}^2 = (\hat{\mathcal{D}}_0^2 + \delta\hat{\Gamma})$ , where  $\hat{\Gamma} = (\hat{\mathcal{D}}_0\hat{\mathcal{D}}_1 + \hat{\mathcal{D}}_1\hat{\mathcal{D}}_0)$ . In an explicit form

$$a^2\hat{\mathcal{D}}_0^2 = -\frac{1}{\sin \theta} \partial_\theta \sin \theta \partial_\theta + \frac{1}{4} + \frac{1}{4 \sin^2 \theta} + \sigma_3 \frac{m - j \cos \theta}{\sin^2 \theta} + \frac{(j - m \cos \theta)^2}{\sin^2 \theta}, \quad (24)$$

and

$$a^2\hat{\Gamma} = 2j^2 - jx(\sigma_3 - 6m) - 4m(m - \sigma_3)x^2 - 2m\sigma_3. \quad (25)$$

Let us write the equation  $\hat{\mathcal{D}}^2\psi = E^2\psi$  by using the appropriate substitution  $x = \cos \theta$  in Eqs.(24) and (25). One obtains

$$[\partial_x(1-x^2)\partial_x - \frac{(j-mx)^2 - j\sigma_3x + \frac{1}{4} + \sigma_3m}{1-x^2} + \delta\hat{\Gamma}] \begin{pmatrix} u_j(x) \\ v_j(x) \end{pmatrix} = -(\lambda^2 - \frac{1}{4}) \begin{pmatrix} u_j(x) \\ v_j(x) \end{pmatrix}, \quad (26)$$

where  $\lambda = aE$ . When  $\delta = 0$ , one has the case of a sphere with magnetic monopole inside. In this case, the exact solution is known (see, e.g., [18])

$$\begin{pmatrix} u_{jn}^0 \\ v_{jn}^0 \end{pmatrix} = \begin{pmatrix} C_u(1-x)^\alpha(1+x)^\beta P_n^{2\alpha, 2\beta}(x) \\ C_v(1-x)^\mu(1+x)^\nu P_n^{2\mu, 2\nu}(x) \end{pmatrix},$$

with the energy spectrum

$$(\lambda_{jn}^0)^2 = (n + |j| + 1/2)^2 - m^2. \quad (27)$$

Here

$$\begin{aligned} \alpha &= \frac{1}{2} \left| j - m - \frac{1}{2} \right|, \beta = \frac{1}{2} \left| j + m + \frac{1}{2} \right|, \\ \mu &= \frac{1}{2} \left| j - m + \frac{1}{2} \right|, \nu = \frac{1}{2} \left| j + m - \frac{1}{2} \right|, \end{aligned} \quad (28)$$

$P_n^{2\alpha, 2\beta}(x)$  and  $P_n^{2\mu, 2\nu}(x)$  are Jacobi polynomials of  $n$ -th order, and  $C_u$  and  $C_v$  are the normalization factors. These states are degenerate. For example, the degeneracy of the zero mode is equal to six. Therefore, we have to use the perturbation scheme for the degenerate energy levels [27]. As a result, the energy spectrum for spheroidal fullerenes is found to be

$$(\lambda_{jn}^\delta)^2 = (n + |j| + 1/2)^2 - m^2 + \delta(2j^2 + jL^1 + jL^2 + L^3 - 2mD_{jn}). \quad (29)$$

Similarly to [18], the possible values of  $j$  obey the condition  $|j| \geq ||m| + 1/2|$  for non-zero modes. Direct calculations show that

$$L^1 = -\frac{j(6m^2 + 1/2)}{p(p+1)} + \frac{jm^2(4m^2 + 5)}{p^2(p+1)^2}, \quad (30)$$

$$L^2 = -\frac{4jmD_{jn}}{p(p+1)} + \frac{jm(8m^2 + 1)D_{jn}}{p^2(p+1)^2}, \quad (31)$$

$$\begin{aligned} L^3 &= 4m(m-1)|C_u|^2 F_n(2\alpha, 2\beta) I_n(2\alpha, 2\beta) \\ &\quad + 4m(m+1)|C_v|^2 F_n(2\mu, 2\nu) I_n(2\mu, 2\nu) \end{aligned} \quad (32)$$

with  $p = n + \beta + \alpha$ ,

$$\begin{aligned} F_n(2\alpha, 2\beta) &= \frac{(n+1)(n+2\alpha+1)(n+2\beta+1)(n+2\alpha+2\beta+1)}{(2p+1)(p+1)^2(2p-n+3)} \\ &\quad + \frac{n(n+2\alpha)(n+2\beta)(n+2\alpha+2\beta)}{(2p-1)p^2(2p+1)}, \end{aligned}$$

$$I_n(2\alpha, 2\beta) = \frac{2^{2\alpha+2\beta+1}\Gamma(n+2\alpha+1)\Gamma(n+2\beta+1)}{n!(2p+1)\Gamma(n+2\alpha+2\beta+1)}, \quad (33)$$

$$D_{jn} = \frac{\Gamma(n+2\mu+1)\Gamma(n+2\nu+1) - \left(\frac{j+1/2}{j-m+1/2}\right)^2 \frac{n+j-m+1/2}{n+j+m+1/2} \Gamma(n+2\alpha+1)\Gamma(n+2\beta+1)}{\Gamma(n+2\mu+1)\Gamma(n+2\nu+1) + \left(\frac{j+1/2}{j-m+1/2}\right)^2 \frac{n+j-m+1/2}{n+j+m+1/2} \Gamma(n+2\alpha+1)\Gamma(n+2\beta+1)} \quad (34)$$

for  $j > 0$  and

$$D_{jn} = \frac{\Gamma(n+2\mu+1)\Gamma(n+2\nu+1) - \left(\frac{|j|+1/2+m}{|j|+1/2}\right)^2 \frac{n+|j|-m+1/2}{n+|j|+m+1/2} \Gamma(n+2\alpha+1)\Gamma(n+2\beta+1)}{\Gamma(n+2\mu+1)\Gamma(n+2\nu+1) + \left(\frac{|j|+1/2+m}{|j|+1/2}\right)^2 \frac{n+|j|-m+1/2}{n+|j|+m+1/2} \Gamma(n+2\alpha+1)\Gamma(n+2\beta+1)} \quad (35)$$

for  $j < 0$ . Finally, in the linear in  $\delta$  approximation, the low energy electronic spectrum of spheroidal fullerenes takes the form

$$E_{jn}^\delta = E_{jn}^0 + E_{jn}^f + E_{jn}^h \quad (36)$$

with

$$E_{jn}^0 = \pm \sqrt{(2\xi+n)(2\eta+n)}, \quad E_{jn}^f = \frac{\delta(2j^2+jL^1)}{2E_{jn}^0}, \quad E_{jn}^h = \frac{\delta(jL^2+L^3-2mD_{jn})}{2E_{jn}^0}, \quad (37)$$

where  $\xi = \mu$  ( $\nu$ ) and  $\eta = \beta$  ( $\alpha$ ) for  $j > 0$  ( $j < 0$ ), respectively. Here we came back to the energy variable  $E = \lambda/a$  (in units of  $\hbar V_F/a$  where  $V_F$  is the Fermi velocity).

Notice that the non-diagonal matrix element of perturbation  $\langle e^{j\phi} | \langle \psi_{jn} | \Gamma | \psi_{-jn} \rangle | e^{-j\phi} \rangle$  turns out to be zero. Therefore, the states with opposite  $j$  do not mix and  $j$  remains a good quantum number as would be expected. As is seen from Eq. (30), for  $\delta = 0$  both eigenstates and eigenvalues are the same as for a sphere (cf. Ref. [18]). At the same time, Eqs. (30)–(35) show that the spheroidal deformation gives rise to an appearance of fine structure in the energy spectrum. The difference in energy between sublevels is found to be linear in  $\delta$  which resembles the Zeeman effect where the splitting energy is linear in magnetic field. In addition we found a further splitting of the states with opposite  $j$ . The splitting is weakly pronounced ('hyperfine' splitting) and entirely dictated by the topological defects. In other words, this splitting is pure topological in its origin. The magnitude of hyperfine splitting is determined by the topological "charge"  $m$ . In particular, for  $m = 0$  (no defects)  $E_{jn}^h = 0$  and no splitting occurs.

Table 1 shows all three contributions (in compliance with Eq. (36)) to the first energy level for various fullerenes with different morphologies. As is clearly seen, the first (double degenerate) level becomes shifted due to spheroidal deformation. Schematically, the structure of the first energy level is shown in Fig.1. The more delicate is the structure of the second level which is presented in Table 2. In this case, the initial (for  $\delta = 0$ ) degeneracy of  $E_{jn}^0$  is equal to six. The spheroidal deformation provokes an appearance of three shifted double degenerate levels (fine structure) which, in turn, are splitted due to the presence of topological defects (see Fig.2). Notice that the magnitude of both shifts and the splitting energy increases with  $j$  and  $m$ . It should be stressed that the experimental observation of such splitting would indicate the presence of topological defects while a measured magnitude of the splitting gives the value of the monopole charge. Notice that in our model we have two possible charges:  $m = g - G = \pm 3/2 - 1$ . For comparison, the model suggested in [24,16] predicts  $m = \pm 3/2$ . Thus, the splitting energy could clarify the proper monopole charge due to topological defects. Notice that a similar small splittings of the spheroidal subshells due to  $D_{5h}$  symmetry was discovered in Ref. [2].

Let us discuss briefly the zero-mode state. As stated above, for a spherical fullerene there is a zero-mode state with a sixfold degeneracy. For spheroidal fullerene, the zero-mode state also exists, however, its degeneracy is twofold. In addition, there appear two slightly shifted "quasi-zero" modes for  $j = \pm 1, \pm 2$ , each of them is also twofold degenerate (there is no hyperfine splitting for quasi-zero-mode states). Indeed, our study shows that in this case  $D_{jn}$  is equal to one, so that  $A_{jn}$  in (30) becomes odd function of  $j$ . It should be stressed that the similar conclusions follow from our analysis based on spheroidal harmonics suggested in Ref. [28]. Thus, we confirm the finding in [2] that there are only up to twofold degenerate states in spheroidal fullerene. Generally, the spheroidal deformation gives rise to a reduction in degeneracy of energy levels in comparison with the spherical case.

### III. CONCLUSION

We have considered the electronic states of spheroidal fullerenes provided the spheroidal deformation from the sphere is small enough. In this case, the spherical representation is used for describing the eigenstates of the Dirac equation, with the slight asphericity considered as a perturbation. The using of the perturbation scheme allows us to find the exact analytical solution of the problem. In particular, the energy spectrum of spheroidal fullerenes is found to possess the fine structure in comparison with the case of the spherical fullerenes. The energy between sublevels is found to be linear in the small distortion parameter  $\delta$  and is positive/negative for prolate/oblate spheroid, respectively. Another principal difference is the obtained hyperfine splitting of the energy levels. We have shown that this splitting is weakly pronounced and entirely dictated by the topological defects, that is it has a topological origin. Our finding confirms the results of [2] that there can exist only up to twofold degenerate states in the  $C_{70}$ .

Notice that for spherical fullerenes ( $\delta = 0$ ) our results agree with those found in [18]. It is interesting that the predictions of the continuum model for spherical fullerenes are in qualitative agreement with tight-binding calculations [29–32]. In particular, the energy gap between the highest-occupied and lowest-unoccupied energy levels becomes more narrow as the size of fullerenes becomes larger. It is important to keep in mind, however, that the continuum model itself is correct for the description of the low-lying electronic states. In addition, the validity of the effective field approximation for the description of big fullerenes is also not clear yet. Actually, this approximation allows us to take into account the isotropic part of long-range defect fields. For bigger fullerenes, one has to consider the anisotropic part of the long-range fields, the influence of the short-range fields due to single disclinations as well as the multiple-shell structure. Therefore, we admit that the proper values of the energy levels can deviate from our estimations.

Finally, the main results obtained for spheroidal fullerenes are the discovery of (i) fine structure with a specific shift of the electronic levels upwards, (ii) hyperfine splitting due to topological defects, and (iii) three twofold degenerate modes near the Fermi level with one of them being the true zero mode. In our opinion, these predictions are quite general for the fullerene family and are of interest for experimental studies.

The work was supported in part by VEGA grant 2/6193/26 of the Slovak Academy of Sciences, by the Science and Technology Assistance Agency under contract No. APVT-51-027904 and by the Russian Foundation for Basic Research under Grant No. 05-02-17721.

- 
- [1] H.W. Kroto, J.R. Heath, S.C.O'Brien, R.F. Curl and R.E. Smalley, *Nature* **318** (1985) 162.
  - [2] S. Saito and A. Oshiyama, *Phys. Rev. B* **44** (1991) 11532.
  - [3] P.E. Lammert and V.H. Crespi, *Phys. Rev. B* **69** (2004) 035406.
  - [4] T. Ando, *J. Phys. Soc. Jpn.* **74** (2005) 777.
  - [5] C. Furtado, F. Moraes, and A.M. de M. Carvalho, *arxiv:cond-mat/0601391*.
  - [6] P.R. Wallace, *Phys. Rev.* **71** (1947) 622.
  - [7] W.H. Lomer, *Proc. Roy. Soc. (London)* **A227** (1955) 330.
  - [8] J.C. Slonczewski and P.R. Weiss, *Phys. Rev.* **109** (1958) 272.
  - [9] J.M. Luttinger and Kohn, *Phys. Rev.* **97** (1955) 869.
  - [10] D.P. DiVincenzo and E.J. Mele, *Phys. Rev. B* **29** (1984) 1685.
  - [11] C.L. Kane and E.J. Mele, *Phys. Rev. Lett.* **78** (1997) 1932.
  - [12] H. Matsumura and T. Ando, *J. Phys. Soc. Jpn.* **67** (1998) 3542.
  - [13] R. Saito, G. Dresselhaus and M.S. Dresselhaus, *Physical Properties of Carbon Nanotubes* (Imperial College Press, London, 2003).
  - [14] V.A. Osipov and E.A. Kochetov, *JETP Lett.* **72** (2000) 199.
  - [15] V.A. Osipov, E.A. Kochetov and M. Pudlak, *JETP* **96** (2003) 140.
  - [16] J. González, F. Guinea and M.A.H. Vozmediano, *Nucl. Phys. B* **406** (1993) 771.
  - [17] J. Tersoff, *Phys. Rev. B* **46** (1992) 15546.
  - [18] D.V. Kolesnikov and V.A. Osipov, *Eur.Phys.Journ. B* **49** (2006) 465.
  - [19] R. Pincak, *Phys. Lett. A* **340** (2005) 267.
  - [20] K. Clemenger, *Phys. Rev. B* **32** (1985) 1359.
  - [21] N.D. Birrell and P.C.W. Davies, *Quantum Fields in Curved Space*, (Cambridge 1982).
  - [22] M. Nakahara, *Geometry, Topology and Physics*, (Institute of Physics Publishing Bristol 1998).
  - [23] M. Göckeler and T. Schücker, *Differential geometry, gauge theories, and gravity* (Cambridge University Press 1989).
  - [24] J. González, F. Guinea and M.A.H. Vozmediano, *Phys. Rev. Lett.* **69** (1992) 172.
  - [25] T.T. Wu and G.N. Yang, *Nucl. Phys. B* **107** (1976) 365.
  - [26] T.T. Wu and G.N. Yang, *Phys. Rev. D* **12** (1975) 3845.
  - [27] L.D. Landau and E.M. Lifshitz, *Quantum Mechanics* (Elsevier Science, Oxford, 2003).
  - [28] E.D. Fackerell and R.G. Crossman, *Journ. of Math. Physics* **18** (1977) 1849.
  - [29] E. Manousakis, *Phys. Rev. B* **44** (1991) 10991.
  - [30] A.Ch. Tang and F.Q. Huang, *Phys. Rev. B* **51** (1995) 13830.
  - [31] A. Perez-Garrido, F. Alhama and J.D. Catala, *Chem. Phys.* **278** (2002) 71.
  - [32] Y.L. Lin and F. Nori, *Phys. Rev. B* **49** (1994) 5020.
  - [33] J. P. Lu and W. Yang, *Phys. Rev. B* **49** (1994) 11421.
  - [34] B. I. Dunlap *et al.*, *J. Phys. Chem.* **95** (1991) 8737.

[35] M. Yoshida and E. Osawa, *Fullerene Sci. Tech.* **1** (1993) 55.



$n = 0, \quad m = 1/2$	$\bar{b}(\text{\AA})$	$\bar{R}(\text{\AA})$	$SD(\text{\AA})$	$\delta$	$j$	$ E_{jn}^0 (eV)$	$ E_{jn}^f (meV)$	$ E_{jn}^h (meV)$
<b>C<sub>180</sub></b>	1.43	6.129	0.075	0.012	1	1.24	5	2.7
					-1	1.24	5	2.2
<b>S-C<sub>240</sub></b>	1.43	7.12	0	0	1	1.07	0	0
					-1	1.07	0	0
<b>YO-C<sub>240</sub></b>	1.45	7.03	0.17	0.024	1	1.094	9	4.6
					-1	1.094	9	3.8
<b>TI-C<sub>240</sub></b>	1.46	7.09	0.18	0.025	1	1.092	10	5
					-1	1.092	10	4
<b>I-C<sub>240</sub></b>	1.45	7.27	0.39	0.054	1	1.06	20	10
					-1	1.06	20	8
<b>S-C<sub>540</sub></b>	1.41	10.5	0	0	1	0.712	0	0
					-1	0.712	0	0
<b>I-C<sub>540</sub></b>	1.43	10.4	0.52	0.05	1	0.729	13	6.4
					-1	0.729	13	5.2

TABLE I. The structure of the first energy level for various fullerenes with different morphologies given in Ref. [33]: S – spherical, I – icosahedron faceted, TI – truncated icosahedron; except C<sub>180</sub> – the structure given in Ref. [34] and YO – given in Ref. [35].  $\bar{b}$  is average bond length,  $\bar{R}$  ( $\bar{R} = a$ ) is average radius,  $SD$  is standard deviation from a perfect sphere (see Refs. [33,34]), so that  $\delta = SD/\bar{R}$ . The hopping integral is taken to be  $t = 2.5 \text{ eV}$  and  $V_F = 3t\bar{b}/2\hbar$ .

<b>YO-C<sub>240</sub></b>	$\bar{b} = 1.45\text{\AA}$	$\bar{R} = 7.03\text{\AA}$	$SD = 0.17\text{\AA}$	$\delta = 0.024$	$j$	$ E_{jn}^0 (eV)$	$ E_{jn}^f (meV)$	$ E_{jn}^h (meV)$
$n = 1, m = 1/2$					1	1.89	6.5	2.5
					-1	1.89	6.5	2.3
$n = 0, m = 1/2$					2	1.89	26	2.2
					-2	1.89	26	1.8
$n = 0, m = -5/2$					3	1.89	4.6	13
					-3	1.89	4.6	18

TABLE II. The structure of the second energy level for YO-C<sub>240</sub>.

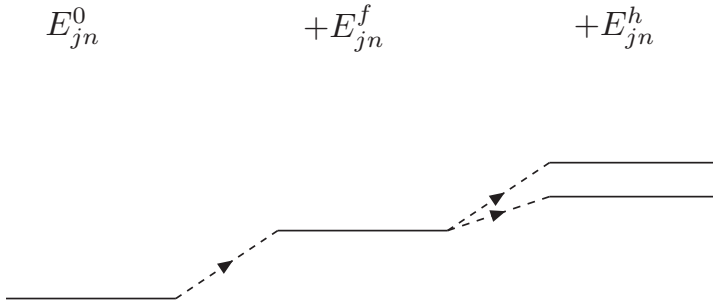


FIG. 1. The schematic picture of the first positive electronic level  $E_{jn}^{\delta}$  for spheroidal fullerenes.

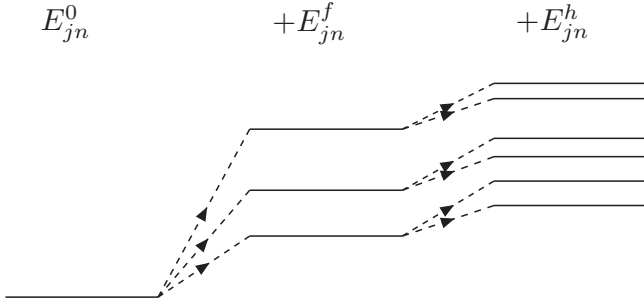


FIG. 2. The schematic picture of the second positive electronic level  $E_{jn}^{\delta}$  for spheroidal fullerenes.